

Optical and Scintillation Properties of Rare-Earth Ion-Doped $12\text{CaO}\cdot 7\text{Al}_2\text{O}_3$ Single Crystals

Narumi Kumamoto,* Daisuke Nakauchi, Takumi Kato,
Go Okada, Noriaki Kawaguchi, and Takayuki Yanagida

Nara Institute of Science and Technology, 8916-5 Takayama, Ikoma, Nara 630-0192, Japan

(Received March 27, 2017; accepted July 18, 2017)

Keywords: single crystal, C12A7, rare earths, scintillation, photoluminescence

We have synthesized undoped and rare-earth (RE)-doped $12\text{CaO}\cdot 7\text{Al}_2\text{O}_3$ (RE:C12A7) crystals by the floating zone (FZ) method to systematically study the effects of RE doping (doped with all the lanthanoid elements except for Sc, Y, La, Pm, and Lu) in C12A7 for radiation detector applications. In both photoluminescence (PL) and scintillation, the undoped C12A7 crystal showed a weak emission due to the lattice defects appearing at around 500 nm, and the decay time was on the order of several nanoseconds. On the other hand, the RE:C12A7 crystals showed PL and scintillation owing to the $4f-4f$ transitions of RE^{3+} ions appearing from the UV to NIR ranges depending on the RE element. The decay times of these emissions ranged from a few microseconds to milliseconds depending on the RE element and the values were typical for the electronic transitions of trivalent rare earths.

1. Introduction

Scintillators are a type of phosphor material and used in radiation detectors for various applications such as security,⁽¹⁾ medical imaging⁽²⁾ and well logging.⁽³⁾ In general, scintillation processes are understood as follows. First, a scintillator absorbs incident radiation energy and generates numerous numbers of electrons and holes. Next, it emits a large number of low-energy [e.g., ultraviolet (UV) and visible] photons immediately via the direct excitation of emission centers by the secondary electrons and recombination of carriers at emission centers.

Rare-earth (RE)-doped bulk crystalline materials are often used as a scintillator since the detection efficiency of detectors simply depends on the volume. The material compositions vary since the cross section of a material against radiation strongly depends on the radiation type. For example, for high-energy photons such as X-rays or γ -rays, materials consisting of heavy elements are suitable since the interaction probabilities increase with increasing density and effective atomic number. On the other hand, those consisting of light elements are appropriate for measuring charged particles such as α -rays since the sensitivity for background X-rays and γ -rays must be low.⁽⁴⁾ In addition, RE ions are often included in the host material in order to enhance the luminescence properties.⁽⁵⁾

In this study, we have synthesized undoped and RE-doped $12\text{CaO}\cdot 7\text{Al}_2\text{O}_3$ (RE:C12A7) single crystals and characterized the properties for scintillator applications. C12A7 is one of the

*Corresponding author: e-mail: kumamoto.narumi.kh6@ms.naist.jp
<http://dx.doi.org/10.18494/SAM.2017.1621>

components of cement.⁽⁶⁾ In the unit cell of C12A7, there are 12 cages with an inner diameter of ~0.4 nm and two different cages hosting extra-framework oxygen ions.⁽⁷⁾ For its wide-band-gap energy of 6.0 eV,⁽⁸⁾ it is transparent in the near-UV and visible ranges, and it has been studied for use in optical devices including conductor devices and transparent displays.^(6–9) In addition, C12A7 is attractive from the viewpoints of cost reduction and resource protection as the components are ubiquitous elements on earth. Until now, photoluminescence (PL) properties of undoped C12A7⁽¹⁰⁾ were reported and RE:C12A7 was also studied in several different material forms: ceramics,^(11–14) powders^(15,16) and single crystals.^(6,17) For radiation detection applications, the thermally stimulated luminescence of Tb-doped C12A7 ceramics and powder forms was also reported,⁽¹⁸⁾ however, no studies can be found for scintillator applications of undoped and RE:C12A7 single crystals.

2. Experimental Procedure

In this study, undoped C12A7 and RE:C12A7 crystal rods were prepared. The concentration of RE ions was fixed to 1.0 mol%. The samples were prepared by using high-purity CaO (99.99%), Al₂O₃ (99.99%), CeO₂ (99.99%), Pr₆O₁₁ (99.99%), Tb₄O₇ (99.99%), and RE₂O₃ (RE = Nd, Sm, Eu, Gd, Dy, Ho, Er, Tm, and Yb; 99.99%) as raw materials. Some RE ions (Sc³⁺, Y³⁺, and La³⁺) were excluded since they have closed-shell structures and do not show electronic transitions to emit luminescence. Also, the 4f orbitals of Lu³⁺ are completely filled, so it also does not show electronic transitions. Pm was excluded for its radioactivity. The synthesis procedures are as follows. First, the starting compounds were well mixed and loaded into a pencil balloon, which was then shaped to a cylinder rod by applying hydrostatic pressure. Second, the obtained rod was sintered at 1100 °C for 10 h in order to obtain a solid ceramic rod. Third, the sintered rod was loaded to a floating zone (FZ) furnace (FZD0192, Canon Machinery Inc.), and the crystal growth was conducted. The heat source used in the instrument was a halogen lamp. The crystal growth rate was 5 mm/h. The obtained crystal rod was cut perpendicular to the crystal growth direction for the measurements described below. Powder X-ray diffraction (XRD) pattern was measured using a diffractometer (MiniFlex 600, RIGAKU) operated at 40 kV and 15 mA scanning the 2θ range of 3–90° and irradiated with a Cu (Kα) X-ray source.

PL emission spectra were measured using a spectrofluorometer (FP-8600, JASCO). The typical wavelength of excitation was selected individually for each RE element. By using Quantaaurus-τ (C11367, Hamamatsu Photonics), the PL decay profile was measured and the decay time was deduced by the least-squares fitting with an exponential decay function. The excitation source was a pulse LED for the measurement of the shorter time range (nanosecond or microsecond) and Xe flash lamp for the longer time range (microsecond or millisecond). For the undoped and Ho-, Er-, and Tm-doped samples, the excitation source was a 365 nm LED and measured over the shorter time range. For the rest of the samples, the measurements were done with the longer time range, and a Xe flash lamp and band-pass filter were used to generate excitation light.

The scintillation spectrum was measured by using our laboratory-constructed setup.⁽¹⁹⁾ The X-ray source used to evaluate the scintillation spectra was a conventional X-ray tube, equipped with a W anode target and Be window (XRB80P&N200X4550, Spellman). The X-ray tube was operated with a bias voltage of 80 kV and tube current of 2.5 mA. We used two CCD-based spectrometers to measure the scintillation spectrum: the Andor DU-420-BU2 with Shamrock SR163 monochromator and the Ocean Optics QE Pro. The former covered the UV to visible range while the latter was used to measure in the near-infrared (NIR) range. The scintillation decay time profile was measured by using our original setup equipped with a pulse X-ray source.⁽²⁰⁾ The

decay time was estimated by approximating with a 1st- or 2nd-order exponential decay function. The data presented for the Pr- and Tb-doped C12A7 were previously reported.^(21,22)

3. Experimental Procedure

The C12A7 crystals grown in this study are shown in Fig. 1. The typical size of an as-grown crystal rod was approximately $4 \text{ mm}\phi \times 20 \text{ mm}$. All the RE-doped crystal rods are in complementary colors of absorption due to the doped RE ion. Under UV excitation at 365 nm, bright emissions from the Sm-, Eu-, Tb-, and Dy-doped samples and weak emissions from the Pr-, Ho-, Er-, and Tm-doped samples were observed by the naked eye. These as-grown crystal rods were cut into a typical size of $4 \text{ mm}\phi \times 2 \text{ mm}$ to extract relatively transparent parts as the Tb-doped samples (Fig. 1).

Figure 2 shows a powder X-ray diffraction pattern of undoped and RE:C12A7 crystals. Each diffraction peak was identified using a reference database of the Joint Committee on Powder Diffraction Standards (JCPDS) (No. 09-0413 of mayenite; C12A7 single crystal, $\text{Ca}_{12}\text{Al}_{14}\text{O}_{33}$ and No. 81-0792 of CeO_2). From this result, we confirmed that the samples, except for the Ce-doped sample, did not contain any impurity phases. The Ce-doped sample contained both mayenite and CeO_2 phases, so Ce was not suitably incorporated into the C12A7 crystal structure under this synthesis condition.

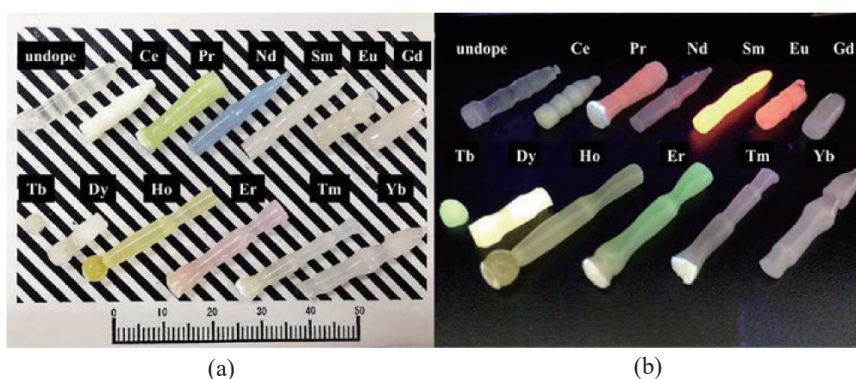


Fig. 1. (Color online) Undoped and RE:C12A7 crystals grown by the FZ method (a) under room light and (b) in the dark under a UV lamp.

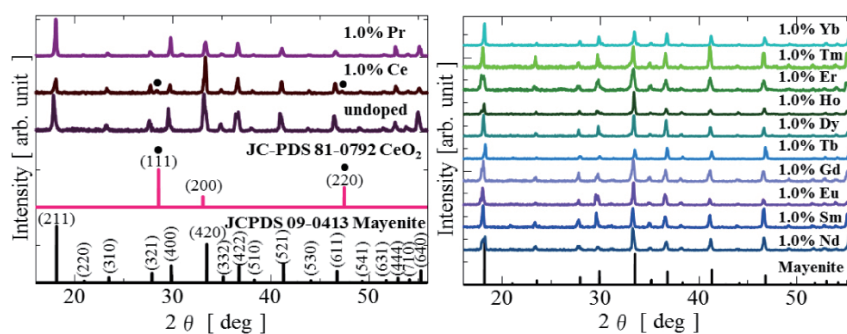


Fig. 2. (Color online) X-ray diffraction pattern of undoped and RE:C12A7 crystals grown by the FZ method.

Figure 3 shows the PL emission spectra of the undoped and RE:C12A7 crystals. The selected excitation wavelength for each measurement was typical for the corresponding RE element and is indicated in the figure. The undoped sample showed a broad emission peaking at around 500 nm. The emission origin is considered to be the lattice defects. On the other hand, samples showed strong emissions with line features. The origins of these emissions are attributed to the corresponding RE ions as the spectral positions and shapes agree with those reported previously but with different hosts.^(23–32) The Ce-, Gd-, and Yb-doped samples did not show any measurable signals. These results can be interpreted as follows. In the Yb-doped sample, Yb³⁺ is known to possess charge transfer luminescence (CTL) in the visible wavelength and the CTL is generally affected by a significant thermal quenching.⁽³³⁾ In the Ce-doped sample, the tetravalent state of Ce would be more stable than the trivalent state in the C12A7 lattice, and Ce⁴⁺ has no electron transition levels. In the Gd-doped sample, the emission intensity was very low. Typically, Gd³⁺

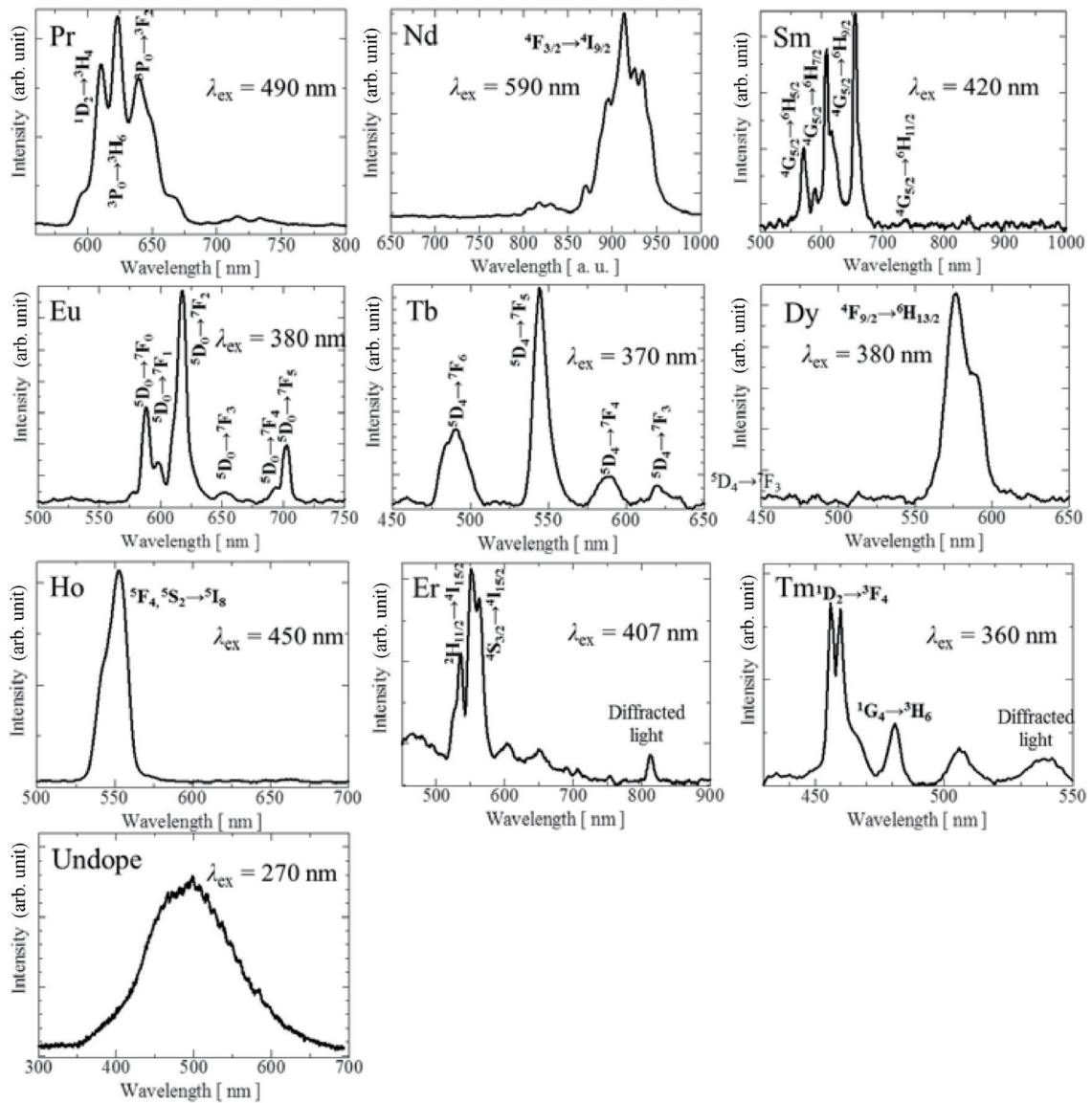


Fig. 3. PL emission spectra of undoped and RE:C12A7 crystals.

is known to show PL emission at around 310 to 270 nm excitation due to the 4f–4f transitions; however, we did not detect any measurable signal. As described later, the scintillation signal was in fact measurable, but the PL internal quantum yield was very low.

Scintillation spectra of the undoped and RE:C12A7 crystals under X-ray irradiation are shown in Fig. 4. The origins of these emission lines were attributed to each trivalent RE ion based on previous studies.^(23–32,34,35) The Ce-doped sample showed no measurable PL emission. Unlike PL, the Gd-doped sample showed a sharp emission line at 310 nm due to the 4f–4f transition of Gd^{3+} . In the Yb-doped sample, no emission peaks were detected in the UV–visible range owing to thermal quenching while a broad band and sharp line emissions were detected in the NIR range from 980 to 1100 nm.

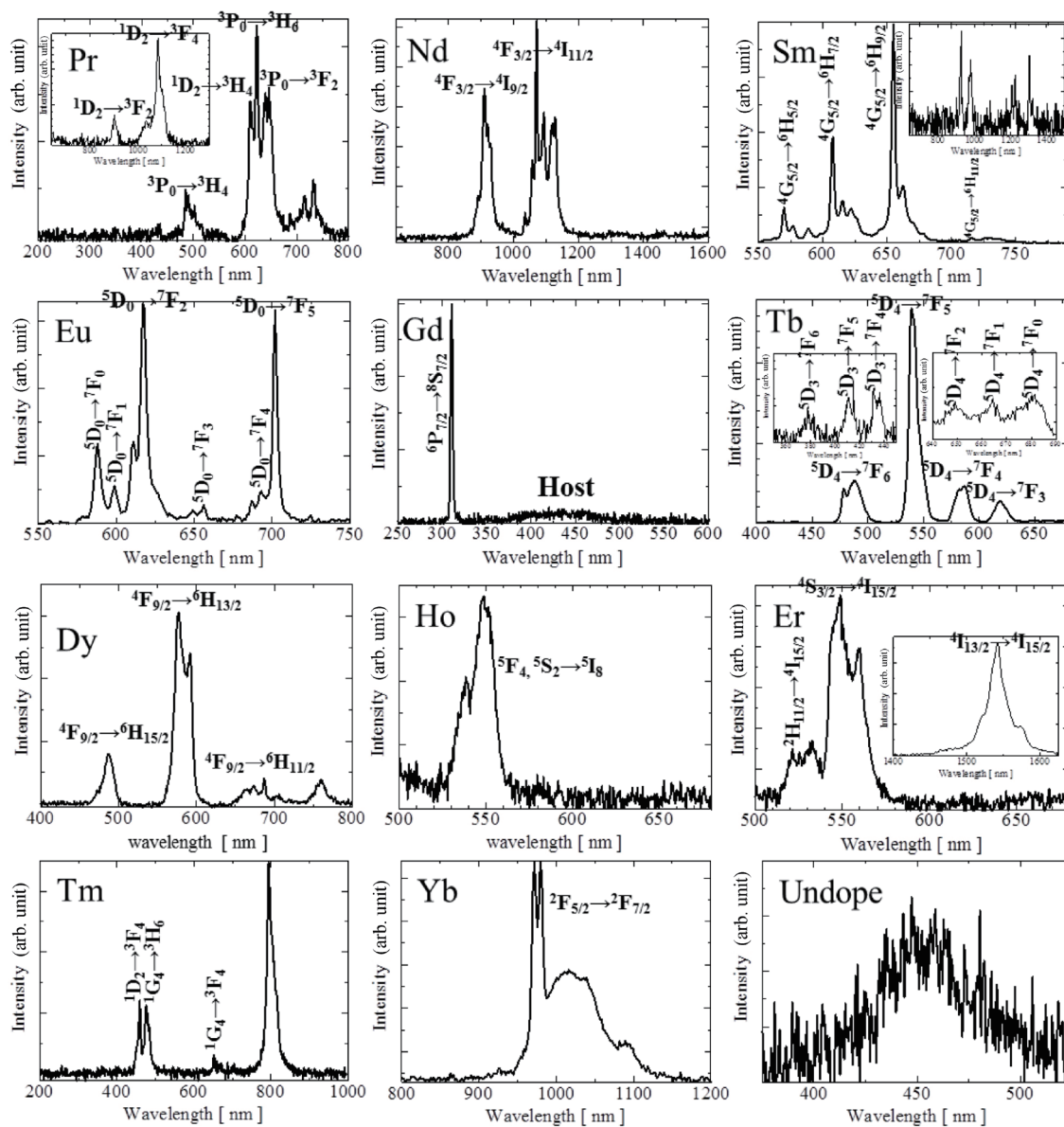


Fig. 4. X-ray induced scintillation spectra of the undoped and RE:C12A7 crystals. The insets for the Pr-, Sm-, and Er-doped samples focus the spectra in the NIR ranges, and the two insets for the Tb-doped samples enlarge the spectrum in the 350–525 and 640–693 nm regions.

Table 1
PL and scintillation decay times of undoped and RE:C12A7 crystals.

Sample	PL excitation/emission wavelength (nm)	PL decay time (ms)	Scintillation decay time (ms)
Undoped	365/450	5.58×10^{-6}	16.3×10^{-6}
Ce	—	—	—
Pr	460–470/600	0.0758	0.0532
Nd	575–625/900	0.379	0.279
Sm	340–390/655	1.58	1.31
Eu	340–390/610	1.99	0.787
Gd	—	—	—
Tb	340–390/530	2.56	1.94
Dy	340–390/580	0.601	0.704
Ho	365/555	0.00260	—
Er	365/554	0.00607	—
Tm	365/457	0.00584	—
Yb	—	—	—

The PL and scintillation decay time profiles of undoped and RE-doped samples are summarized in Table 1. In the analysis, the instrumental response was deconvoluted in the undoped sample, and we fit the tail part of the decay curves of all the other samples since we could not precisely measure the instrumental response in μs and ms time ranges. In PL, the undoped sample showed the fastest signal with decay times shorter than 10 ns. For the RE-doped samples, all the deduced decay times were typical values of 4f–4f transitions of each trivalent RE ion.^(24,31,36,37) The Ho-doped sample showed the fastest decay time among the RE-doped samples.

On the other hand, in the scintillation, the scintillation decay curves of Gd-, Ho-, Er-, Tm-, and Yb-doped samples could not be detected. The undoped sample also showed the fastest decay time, as for PL. The decay time constant derived for all the RE-doped samples were due to 4f–4f transitions of RE^{3+} ions.^(24,38,39) In the Pr-, Nd-, Sm-, Eu- and Tb-doped samples, the decay time constants were shorter than those of PL. In general, the decay time constants of PL are shorter than that of scintillation since the scintillation process involves energy migration processes in addition to simple excitation/emission processes.⁽⁴⁰⁾ A typical interpretation is as follows. During the scintillation processes, energetic secondary electrons migrate in the matrix, and the energy is transferred to the luminescent center or quenched by interacting with each other. When the quenching process is predominantly involved, the decay time tends to be shortened. We expect that the same processes are involved in the present samples.

4. Conclusions

We synthesized undoped and RE:C12A7 single crystals by the FZ method and investigated the PL and scintillation properties. In the PL and scintillation spectra, emissions due to the lattice defects of the host and 4f–4f transitions of RE^{3+} ions were detected in the UV, visible and NIR ranges. The decay time constants of the RE-doped samples in both PL and scintillation were a few microseconds or milliseconds due to the 4f–4f transitions of RE^{3+} ions. The decay time constant of the undoped sample was on the order of nanoseconds and appeared to be the shortest among the samples studied in this research.

Acknowledgments

This work was supported by a Grant-in-Aid for Scientific Research (A) 26249147 from the Ministry of Education, Culture, Sports, Science and Technology of Japan (MEXT) and partially by JST A-step. The Cooperative Research Project of the Research Institute of Electronics, Shizuoka University, Inamori Foundation and KRF Foundation are also acknowledged.

References

- 1 D. Totsuka, T. Yanagida, K. Fukuda, N. Kawaguchi, Y. Fujimoto, Y. Yokota, and A. Yoshikawa: Nucl. Instrum. Methods Phys. Res., Sect. A **659** (2011) 399.
- 2 T. Yanagida, A. Yoshikawa, Y. Yokota, K. Kamada, Y. Usuki, S. Yamamoto, M. Miyake, M. Baba, K. Kumagi, K. Sasaki, M. Ito, N. Abe, Y. Fujimoto, S. Maeo, Y. Furuya, H. Tanaka, A. Fukabori, T. R. D. Santos, M. Takeda, and N. Ohuchi: IEEE Nucl. Trans. Sci. **57** (2010) 1492.
- 3 T. Yanagida, Y. Fujimoto, S. Kurosawa, K. Kamada, H. Takahashi, Y. Fukazawa, M. Nikl, and V. Chani: Jpn. J. Appl. Phys. **52** (2013) 076401.
- 4 T. Yanagida, Y. Fujimoto, M. Miyamoto, and H. Sekiwa: Jpn. J. Appl. Phys. **53** (2014) 02BC13.
- 5 T. Yanagida: Opt. Mater. **35** (2013) 1987.
- 6 E. Feizi and A. K. Ray: J. Dis. Technol. **12** (2016) 451.
- 7 M. Miyakawa, S. W. Kim, M. Hirano, Y. Kohama, H. Kawaji, T. Atake, H. Ikegami, K. Kono, and H. Hosono: J. Am. Chem. Soc. **129** (2007) 7270.
- 8 P. V. Shusko, A. L. Shluger, K. Hayashi, M. Hirano, and H. Hosono: Phys. Rev. Lett. **91** (2003) 126401.
- 9 Y. Toda, M. Miyakawa, K. Hayashi, T. Kamiya, M. Hirano, and H. Hosono: Thin Solid Films **445** (2003) 309.
- 10 E. Feldbach, V. P. Denks, M. Kirm, K. Kunnus, and A. Maaros: Radiat. Meas. **45** (2010) 281.
- 11 E. Töldsepp, E. Feldbach, and M. Kirm: J. Ceram. Soc. Tech. **4** (2013) 77.
- 12 X. Zhang, Y. Liu, M. Zhang, J. Yang, H. Zhu, D. Yan, C. Liu, and C. Xu: Mater. Res. Bull. **86** (2017) 51.
- 13 S. Liao, R. Yao, Y. Liu, X. Chen, X. Hu, and F. Zheng: J. Alloys Compd. **642** (2015) 7.
- 14 R. Wang, L. Liu, J. Sun, Y. Qian, Y. Zhang, and Y. Xu: Opt. Commun. **285** (2012) 957.
- 15 Y. X. Liu, L. Ma, D. T. Yan, H. C. Zhu, X. L. Liu, H. Y. Bian, H. Zhang, and X. J. Wang: J. Lumin. **152** (2014) 28.
- 16 Z. Hancheng, L. Yuxue, Y. Duanting, Y. Xiaolei, L. Chunguang, and X. Changshan: J. Nanosci. Nanotechnol. **11** (2011) 9958.
- 17 M. M. Ali, M. Nagao, S. Watauchi, and I. Tanaka: ACS Omega **1** (2016) 1157.
- 18 P. L. C. Filho, R. L. A. T. Menezes, and W. M. Azevedo: Radiat. Meas. **71** (2014) 65.
- 19 T. Yanagida, K. Kamada, Y. Fujimoto, H. Yagi, and T. Yanagitani: Opt. Mater. **35** (2013) 2480.
- 20 T. Yanagida, Y. Fujimoto, T. Ito, K. Uchiyama, and K. Mori: Appl. Phys. Exp. **7** (2014) 062401.
- 21 N. Kumamoto, D. Nakauchi, T. Kato, G. Okada, N. Kawaguchi, and T. Yanagida: Optik **131** (2017) 957.
- 22 N. Kumamoto, D. Nakauchi, T. Kato, G. Okada, N. Kawaguchi, and T. Yanagida: J. Rare Earths (in press).
- 23 A. I. Voloshin, N. M. Shavaleev, and V. P. Kazakov: J. Lumin. **93** (2001) 199.
- 24 D. Nakauchi, G. Okada, M. Koshimizu, and T. Yanagida: J. Rare Earths **34** (2016) 757.
- 25 C. Koughia, A. Edgar, C. R. Varoy, G. Okada, H. v. Seggern, G. Belev, C. Y. Kim, R. Sammynaiken, and S. Kasap: J. Am. Ceram. Soc. **94** (2011) 543.
- 26 R. P. Merino, A. C. Gallardo, M. G. Rocha, I. H. Calderon, V. Castano, and R. Rodriguez: Thin Solid Films **401** (2001) 118.
- 27 C. A. Kodaira, H. F. Brito, E. E. S. Teotonio, M. C. F. C. Felinto, O. L. Malta, and G. E. S. Brito: J. Braz. Chem. Soc. **15** (2004) 890.
- 28 K. Riwotzki and M. Haase: J. Phys. Chem. B **102** (1998) 10129.
- 29 W. J. Zhang, D. C. Yu, J. P. Zhang, Q. Qian, S. H. Xu, Z. M. Yang, and Q. Y. Zhang: Opt. Mater. Express **2** (2012) 636.
- 30 A. J. Steckl and R. Birkhahn: Appl. Phys. Lett. **73** (1998) 1700.
- 31 H. Zhu, Y. Liu, D. Zhao, M. Zhang, J. Yang, D. Yan, C. Liu, C. Xu, C. Layfield, L. Ma, and X. Wang: Opt. Mater. **59** (2016) 55.
- 32 K. L. Frindell, M. H. Bartl, M. R. Robinson, G. C. Bazan, A. Popitsch, and G. D. Stucky: J. Solid State Chem. **172** (2003) 81.

- 33 T. Yanagida, Y. Fujimoto, H. Yagi, and T. Yanagitani: *Opt. Mater.* **36** (2014) 1044.
- 34 J. Liu, X. Ge, L. Sun, R. Wei, J. Liu, and L. Shi: *RSC Adv.* **6** (2016) 47427.
- 35 V. Singh, S. Borkotoky, A. Murali, J. L. Rao, T. K. G. Rao, and S. J. Dhoble: *Acta A Mol: Biomol. Spectrosc.* **139** (2015) 1.
- 36 Y. Chen, J. Wang, C. Liu, J. Tang, X. Kuang, M. Wu, and Q. Su: *Opt. Express* **21** (2013) 3161.
- 37 H. Wang, J. Yang, C. M. Zhang, and J. Lin: *J. Solid State Chem.* **182** (2009) 2716.
- 38 M. Nikl, P. Bohacek, A. Vedda, M. Fasoli, J. Pejchal, A. Beitlerova, M. Fraternali, and M. Livan: *J. Appl. Phys.* **104** (2008) 093514.
- 39 T. Kuro, G. Okada, N. Kawaguchi, Y. Fujimoto, H. Masai, and T. Yanagida: *Opt. Mater.* **62** (2016) 561.
- 40 M. Koshimizu, K. Iwamatsu, M. Taguchi, S. Kurashima, A. Kimura, T. Yanagida, Y. Fujimoto, K. Watanabe, and K. Asai: *J. Lumin.* **169** (2016) 678.